CD169-CD43 interaction is involved in erythroblastic island formation and erythroid differentiation

Jian Bai,[1]* Fan Fan,[1]* Chunchen Gao,[1]* Shaohua Li,[2]* Wei Li,[3] Tiaoxia Wei,[1] Shilin Cheng,[1] Jinmin Yu,[1] Chao Zheng,[1] Junlong Zhao,[1] Linru Zou,[1] Lei Feng,[1] Jing Yi[4] and Hongyan Qin[1]

[1]State Key Laboratory of Cancer Biology, Department of Medical Genetics and Developmental Biology, Fourth Military Medical University, Xi'an; [2]Department of Aerospace Physiology, Fourth Military Medical University, Xi'an; [3]Department of Hematology, The First Affiliated Hospital of Zhengzhou University, Zhengzhou and [4]Department of Transfusion Medicine, Xijing Hospital, Fourth Military Medical University, Xi'an, Shaanxi, China

**JB, FF, CG and SL contributed equally as first authors.*

Correspondence: H. Qin
hyqin@fmmu.edu.cn

Received: September 28, 2022.
Accepted: February 23, 2023.
Early view: March 2, 2023.

https://doi.org/10.3324/haematol.2022.282192

Supplementary Methods

Quantitative RT-PCR

The total RNA was extracted from BMDMs using TRIzol reagent (Invitrogen), cDNA was synthesized using the HiScript II Q RT SuperMix kit (Vazyme), and qRT-PCR was performed with the ChamQ SYBR qPCR Master Mix kit (Vazyme) by utilizing the ABI PRISM 7500 Real-time PCR system (Life Technologies) with β-actin as internal controls. The primers for CD169 and β-actin were as follows: CD169-F: AGTGATAGCAACCGCTGGTTA; CD169-R: GCACAGGTAGGGTGTGGAAC; Actin-F: CATCCGTAAAGACCTCTATGCCAAC; and Actin-R: ATGGAGCCACCGATCCACA.

Immunofluorescence

BMDMs were fixed and stained with rabbit anti-mouse F4/80 (Servicebio) and rat anti-mouse CD169 antibodies (Biorad) for 12 h. Alexa Fluor 488-conjugated donkey anti-rat IgG (H+L) (Invitrogen) and Cy3-conjugated goat anti-rabbit IgG (H+L) (Boster) were used as secondary antibodies. Images were captured with a Nikon ECLIPSE NI Imaging System (Nikon, Japan).

Hemin-induced K562 cells towards erythroid differentiation

Human erythroleukemia K562 cells were purchased from the ATCC repository and preserved in our lab. K562 cells were cultured in Roswell Park Memorial Institute (RPMI) 1640 medium with 10% fetal bovine serum (FBS, ExCell, FSS500) and induced by 40 μM hemin (MCE) toward erythroid differentiation. The effect of recombinant human Siglec1 protein (RD) on K562 differentiation was also observed. The degree of erythroid differentiation was evaluated by benzidine staining and FACS assay with CD235a and CD43 staining.

Recombinant Siglec1 protein binding assay

BM EBs were sorted by FACS using BD AriaIIa, then treated with recombinant mouse Siglec1-Fc and Fc protein at $1x10^6$ cells per mg at 37 °C for 1 h in PBS plus 2% FBS without EDTA medium. The binding was measured by staining with PE anti-mouse CD169 (Invitrogen) or DyLight 488 anti-mouse Fc antibody (Abcam) by flow cytometery.

Blood parameter measurement

After anesthesia, the peripheral blood from the mice was collected into a tube containing K2EDTA for a complete blood count using Sysmex XN-1000V (Sysmex, Japan).

Lentivirus overexpression of VCAM-1 in cultured BMDMs

Mouse BMDMs were prepared and infected with control or VCAM-1-overexpressing lentiviruses at a multiplicity of infection (MOI) of 50 (Shanghai GeneChem) for 36 h at 37 °C in the presence of 1× HitransG A. Then BMDMs were cultured in fresh medium for 36 h for further analysis and experiment.

The analyses of EBI macrophages nursing cell phenotype

$CD11b^{lo}F4/80^{+}$ BM macrophages were sorted from CD169 WT and CD169 KO mice respectively, and cells were lysed in TRIzol. The RNA sequencing was performed on Illumina Novaseq6000 by Gene Denovo Biotechnology Co. Ltd. (Guangzhou, China) (Data not shown). The nursing cell phenotype of EBI macrophages was determined with genes supporting erythropoiesis between CD169 WT and KO BM macrophages, such as molecules including adhesion, nucleus engulfment, iron handling, transcription factors, growth factors, and membrane receptors.

Supplementary Table

Table S1. Antibody list. Antibodies used in this study.

Supplementary Figure legends

Figure S1. Overexpression of VCAM-1 on BMDMs might not rescue the impairment of EBI formation *in vitro* upon blocking CD169. (A) The schematic procedure of EBI formation in vitro. BMDMs pretreated with IgG isotype or anti-CD169 antibody were mixed with sorted BM EBs at 1:20 ratio and cocultured for 12 hours followed by cytospin analyses. **(B)** The purity of sorted BM EBs was confirmed by FACS. **(C)** The CD169 and VCAM-1 expression of $CD11b^{+}F4/80^{+}$ macrophages were analyzed by FACS. **(D)** Lentivirus-mediated VCAM-1 overexpression in BMDMs was detected by FACS. **(E)** Sorted BM EBs were co-cultured with control and VCAM-1 overexpressed BMDMs pretreated with anti-CD169 antibody, then in vitro EBI formation was examined by MGG staining (n = 3). **(F)** Quantitative analyses of *in vitro* EBI formation by the percentage of various numbers of surrounding EBs associated with BMDMs in (E) (n = 3). **(G)** The binding ability of recombinant mouse CD169-Fc protein to sorted BM EBs was examined by FACS with recombinant mouse Fc protein as control stained by anti-mouse Fc antibody (n = 3). **(H)** The MUC1 and CD43 expression of sorted BM EBs was detected by western blot. Data were shown as mean ± SEM.

Figure S2. CD169 deficiency is negligible to hematopoietic stem and progenitor cells development. (A) The genotypes of CD169-CreERT mice were determined by PCR. **(B)** The percentage and cell numbers of macrophages in the BM were quantitatively analyzed as shown in (Figure 2B). **(C)** Representative flow cytometry analysis of BM hematopoietic stem and progenitor cells from CD169 WT and KO mice. **(D)** The percentage and cell numbers of hematopoietic stem and various progenitor cells in the BM were calculated and quantitatively compared between CD169 WT and KO mice. **(E)** No tdTomato expression was detected in T cells, B cells and NK cells of $CD169\text{-}CreERT^{+/-}$ $ROSA26\text{-}tdTomato^{+/-}$ mice (n = 3). Data were shown as mean ± SEM.

Figure S3. Hemin induces K562 cells towards erythroid differentiation with increased positive benzidine staining and CD235a expression as well as decreased CD43 expression. (A) The MFI of CD43 at various stages of BM EBs differentiation in (Figure 3A) was quantitatively compared by Tukey's multiple comparison test (n = 14). **(B)** Pearson's correlation between CD43 and CD44 expression of BM EBs at distinct stages measured using MFI is illustrated in a scatter plot. **(C-F)** K562 cells were treated with DMSO control or hemin for 24, 48, 72, 96 hours. The positive cell rate of benzidine staining **(C)**, the percentage of $CD235a^+$ K562 cells **(D)**, as well as the CD43 MFI and RFI of K562 cells **(E and F)** were determined and quantitively compared between DMSO control and hemin group at different time points (n = 3). Data were shown as mean ± SEM; *p < 0.05; **p < 0.01; ***p < 0.001.

Figure S4. CD169 deletion could not influence other adhesion molecules expression in BM EBIs and spleen homeostatic erythropoiesis. (A) CD43 expression of $CD45^-CD11b^-Ter119^+$ BM EBs as shown in (Figure 5D) was detected by FACS from CD169 WT and KO mice, and the MFI of CD43 was quantitatively compared. **(B)** Representative histograms showing VCAM-1 and αV expression of EBI central macrophages and their positive percentages in CD169 WT and KO mice. **(C and D)** The expression of integrin α4 and integrin β1 on total EBs (C) and Pro-EBs (D) in BMs of CD169 WT and KO mice was analyzed by FACS. **(E)** Representative photograph of spleen dissected from CD169 WT and KO mice. **(F)** Quantification of spleen weight in CD169 WT and KO mice. **(G)** Representative flow cytometry gating strategy of spleen EBs from CD169 WT and KO mice. **(H)** The percentage and cell numbers of spleen EBs as shown in (G) were quantitatively compared between CD169 WT and KO mice. **(I)** The percentage of spleen EBs at different stages of EBs development in (G) was quantitatively compared. **(J)** The CD43 expression of $CD45^-CD11b^-Ter119^+$ spleen EBs as shown in (G) was detected by FACS from CD169 WT and KO mice, and the MFI of CD43 was quantitatively compared. **(K)** The CD169 expression on spleen macrophages was analyzed by FACS in CD169 WT and KO mice,

respectively. **(L)** The percentage and cell numbers of spleen RPM and MZM in (K) were quantitatively compared. **(M)** RBC, hematocrit (HCT), and hemoglobin (HGB) measurement in peripheral blood of CD169 WT and KO mice (n = 3). Data were shown as mean ± SEM.

Figure S5. CD169 deletion might not affect EBI nursing macrophage phenotype based on RNA sequencing data. (A) The FPKM value of adhesion molecules involved in macrophage-erythroblast interaction. **(B)** The FPKM value of nucleus engulfment associated genes as indicated. **(C)** The FPKM value of iron handling genes as indicated. **(D)** The FPKM value of transcription factors as indicated. **(E)** The FPKM value of growth factors as indicated. **(F)** The FPKM value of membrane receptors as indicated. Data are shown as mean ± SEM (n = 3).

Figure S6. Enhanced BM and spleen stress erythropoiesis in HAPC mice. (A) RBC, hematocrit (HCT), and hemoglobin (HGB) measurement in peripheral blood of WT control and HAPC mice. **(B)** Representative photograph of femurs dissected from control and HAPC mice. **(C)** The CD169 expression in EBIs gated as $Ter119^{+}F4/80^{+}$ live multiplets was determined by FACS from control and HAPC mice, respectively. **(D)** The percentage of BM EBIs and CD169 MFI in control and HAPC mice as shown in (C) were quantitatively compared. **(E)** Representative flow cytometry gating strategy of BM EBs from control and HAPC mice. **(F)** The percentage and cell numbers of BM EBs as shown in (E) were quantitatively compared between control and HAPC mice. **(G)** The percentage of BM EBs at distinct stages of EBs differentiation as shown in (E) was quantitatively compared. **(H)** The CD169 expression on BM macrophages was determined by FACS from control and HAPC mice, respectively. **(I)** The percentage and cell numbers of macrophages and monocytes in (H) were quantitatively compared. **(J)** Representative photograph of spleen dissected from control and HAPC mice. **(K)** Quantification of spleen weight in control and HAPC mice. **(L)** Representative flow cytometry gating strategy of spleen EBs from control and HAPC mice. **(M)** The

percentage and cell numbers of spleen EBs as shown in (L) were quantitatively compared between control and HAPC mice. **(N)** The percentage of spleen EBs at different stages of EBs development in (L) was quantitatively compared between control and HAPC mice. **(O)** The CD169 expression on spleen macrophages was analyzed by FACS in control and HAPC mice, respectively. **(P)** The percentage and cell numbers of spleen RPM and MZM in (O) were quantitatively compared in control and HAPC mice (n = 3). Data were shown as mean ± SEM; *p < 0.05; **p < 0.01; ***p < 0.001.

Figure S7. CD169 is not required for spleen stress erythropoiesis in HAPC. (A) Representative photograph of femurs dissected from CD169 WT and KO HAPC mice. **(B)** CD169 expression on BM macrophages was determined by FACS from CD169 WT and KO HAPC mice, respectively. **(C)** The percentage and cell numbers of macrophages and monocytes in (B) were quantitatively compared (n = 6). **(D)** Representative photograph of spleen dissected from CD169 WT and KO HAPC mice. **(E)** Quantification of spleen weight in CD169 WT and KO HAPC mice (n = 6). **(F)** Representative flow cytometry gating strategy of spleen EBs from CD169 WT and KO HAPC mice. **(G)** The percentage and cell numbers of spleen EBs as shown in (F) were quantitatively compared between CD169 WT and KO HAPC mice (n = 6). **(H)** The percentage of spleen EBs at different stages of EBs development in (F) was quantitatively compared between CD169 WT and KO HAPC mice (n = 6). **(I)** The CD43 expression of $CD45^{-}CD11b^{-}Ter119^{+}$ spleen EBs as shown in (F) was detected by FACS from CD169 WT and KO HAPC mice, and the MFI of CD43 was quantitatively compared (n = 4). **(J)** The CD169 expression on spleen macrophages was analyzed by FACS in CD169 WT and KO HAPC mice, respectively. **(K)** The percentage and cell numbers of spleen RPM and MZM in (J) were quantitatively compared in CD169 WT and KO HAPC mice (n = 6). **(L)** RBC, hematocrit (HCT), and hemoglobin (HGB) measurement in peripheral blood of CD169 WT and KO HAPC mice (n = 6). Data were shown as mean ± SEM; *p < 0.05.

Figure S8. CD169 slightly promotes erythroid differentiation in hemin-induced K562 cells. K562 cells were treated with hemin or hemin+CD169 for 24, 48, 72, 96 hours. The positive cell rate of benzidine staining **(A)**, the percentage of $CD235a^+$ K562 cells **(B)**, as well as the CD43 MFI and RFI of K562 cells **(C and D)** were determined and quantitively compared between hemin and hemin+CD169 group at different time points (n = 3). Data were shown as mean ± SEM; *p < 0.05; **p < 0.01.

Figure S1

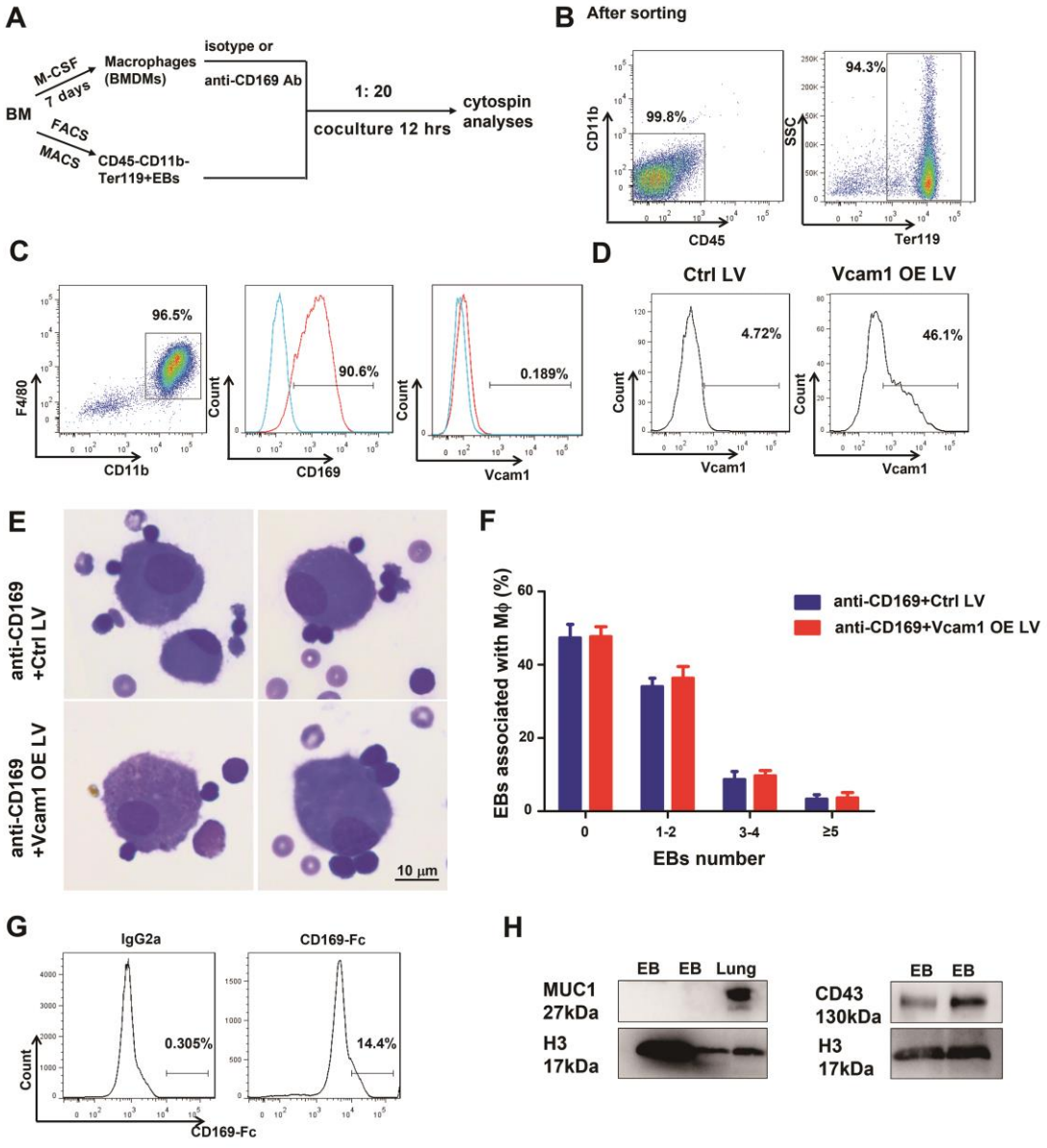
A
BM
M-CSF
7 days
Macrophages (BMDMs)
FACS
MACS
CD45-CD11b-Ter119+EBs
isotype or
anti-CD169 Ab
1: 20
coculture 12 hrs
cytospin analyses
B
After sorting
99.8%
CD11b
CD45
94.3%
SSC
Ter119
C
96.5%
F4/80
CD11b
Count
90.6%
CD169
0.189%
Vcam1
D
Ctrl LV
Vcam1 OE LV
4.72%
46.1%
Count
Vcam1
E
anti-CD169 +Ctrl LV
anti-CD169 +Vcam1 OE LV
10 μm
F
EBs associated with Mϕ (%)
anti-CD169+Ctrl LV
anti-CD169+Vcam1 OE LV
0
1-2
3-4
≥5
EBs number
G
IgG2a
CD169-Fc
0.305%
14.4%
Count
CD169-Fc
H
EB EB Lung
MUC1 27kDa
H3 17kDa
EB EB
CD43 130kDa
H3 17kDa

Figure S2

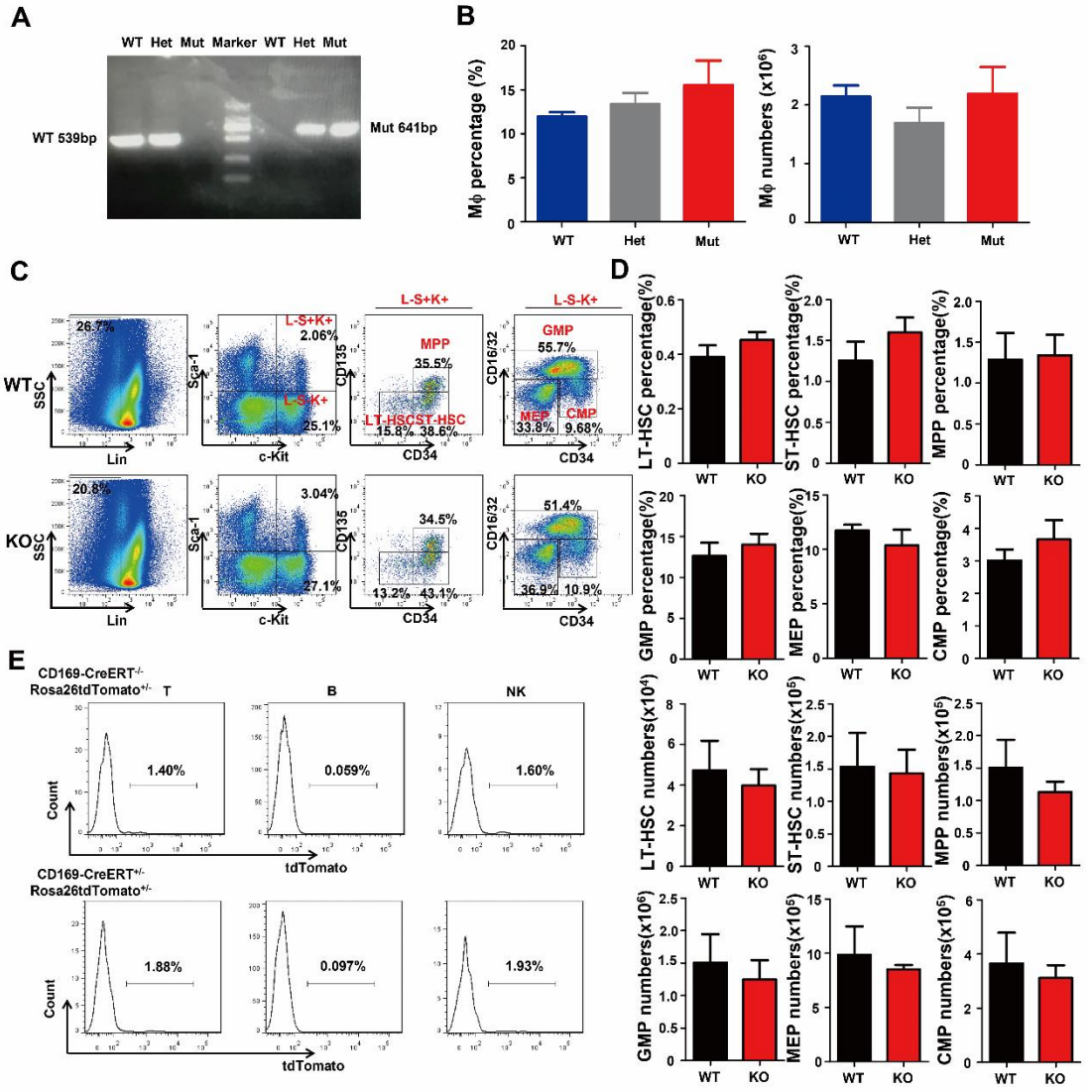
A
WT Het Mut Marker WT Het Mut
WT 539bp
Mut 641bp
B
Mϕ percentage (%)
Mϕ numbers (x10⁶)
WT
Het
Mut
C
WT
KO
SSC
Lin
Sca-1
c-Kit
CD135
CD34
CD16/32
L-S+K+
L-S-K+
26.7%
2.06%
25.1%
35.5%
15.8%
38.6%
55.7%
33.8%
9.68%
20.8%
3.04%
27.1%
34.5%
13.2%
43.1%
51.4%
36.9%
10.9%
D
LT-HSC percentage(%)
ST-HSC percentage(%)
MPP percentage(%)
GMP percentage(%)
MEP percentage(%)
CMP percentage(%)
LT-HSC numbers(x10⁴)
ST-HSC numbers(x10⁵)
MPP numbers(x10⁵)
GMP numbers(x10⁶)
MEP numbers(x10⁵)
CMP numbers(x10⁵)
E
CD169-CreERT-/-
Rosa26tdTomato+/-
CD169-CreERT+/-
Rosa26tdTomato+/-
T
B
NK
1.40%
0.059%
1.60%
1.88%
0.097%
1.93%
Count
tdTomato

Figure S3

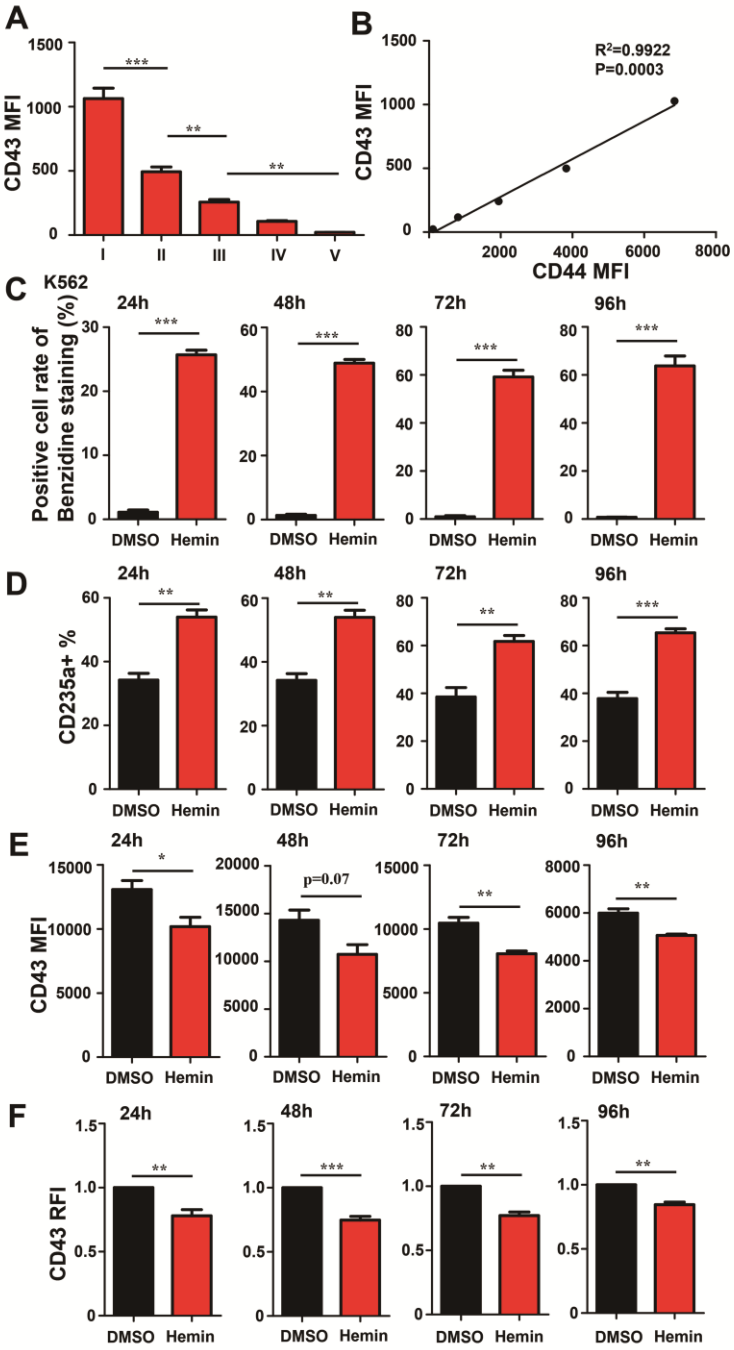
A
CD43 MFI
1500
1000
500
0
***
**
**
I
II
III
IV
V
B
CD43 MFI
R²=0.9922
P=0.0003
CD44 MFI
2000
4000
6000
8000
C
K562
Positive cell rate of Benzidine staining (%)
24h
48h
72h
96h
***
DMSO
Hemin
D
CD235a+ %
**
***
E
CD43 MFI
*
p=0.07
F
CD43 RFI

Figure S4

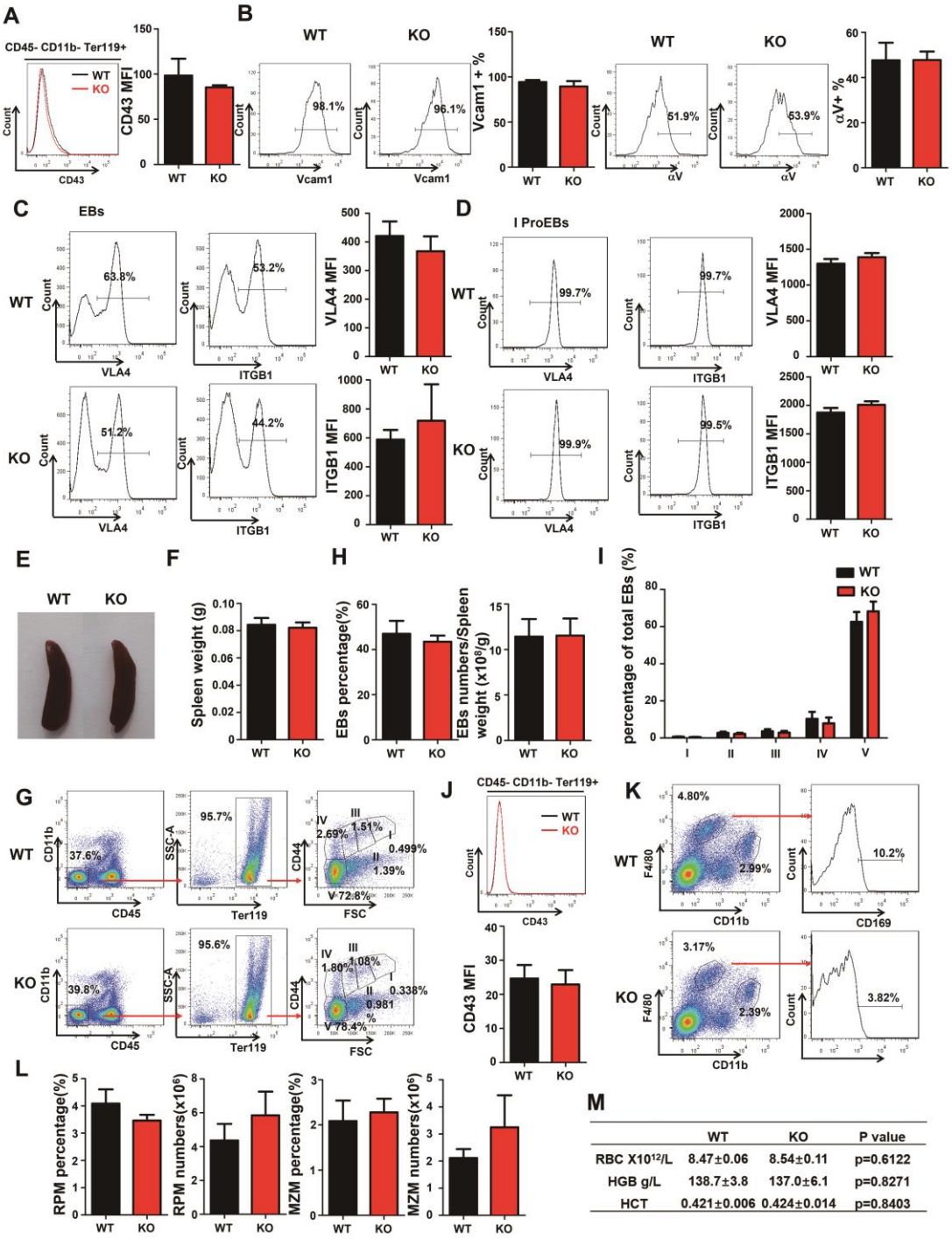
A
CD45- CD11b- Ter119+
WT
KO
Count
CD43
CD43 MFI
B
WT
KO
98.1%
96.1%
Vcam1
Vcam1 + %
51.9%
53.9%
αV
αV+ %
C
EBs
63.8%
53.2%
51.2%
44.2%
VLA4
ITGB1
VLA4 MFI
ITGB1 MFI
D
I ProEBs
99.7%
99.9%
99.5%
E
F
Spleen weight (g)
H
EBs percentage(%)
EBs numbers/Spleen weight (x10⁸/g)
I
percentage of total EBs (%)
I
II
III
IV
V
G
37.6%
95.7%
2.69%
1.51%
0.499%
1.39%
72.6%
39.8%
95.6%
1.80%
1.08%
0.338%
0.981
78.4%
CD11b
CD45
SSC-A
Ter119
CD44
FSC
J
CD45- CD11b- Ter119+
CD43
CD43 MFI
K
4.80%
2.99%
10.2%
3.17%
2.39%
3.82%
F4/80
CD169
L
RPM percentage(%)
RPM numbers(x10⁶)
MZM percentage(%)
MZM numbers(x10⁶)
M

	WT	KO	P value
RBC X10¹²/L	8.47±0.06	8.54±0.11	p=0.6122
HGB g/L	138.7±3.8	137.0±6.1	p=0.8271
HCT	0.421±0.006	0.424±0.014	p=0.8403

Figure S5

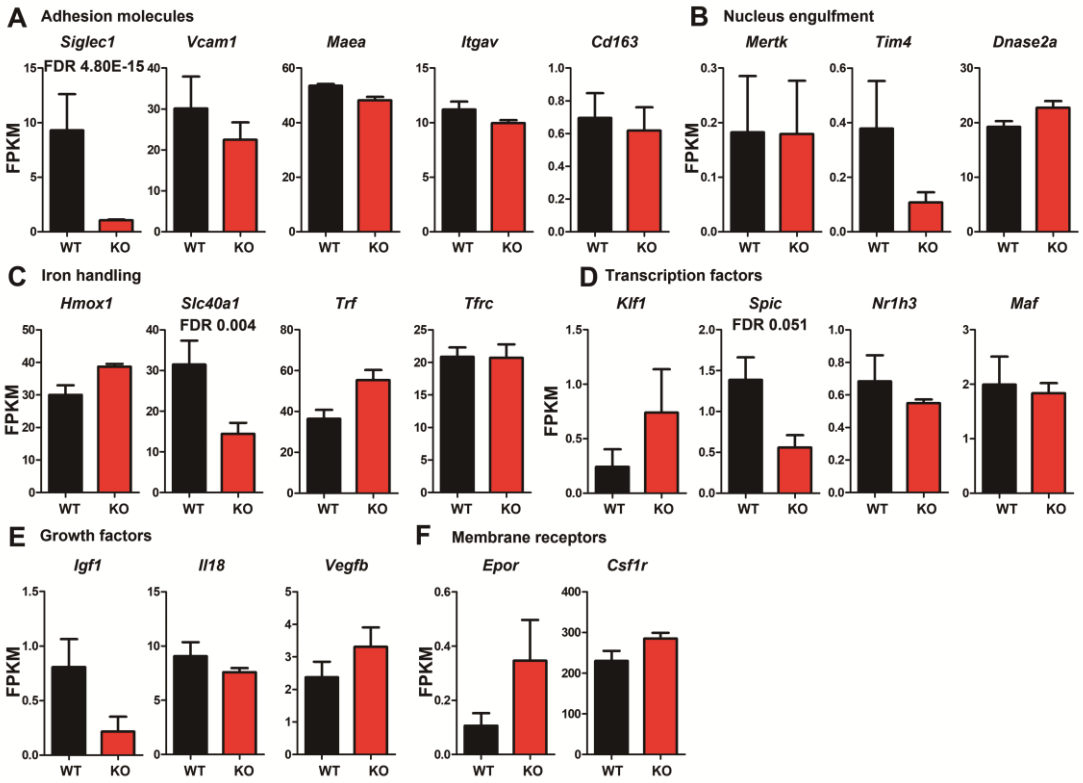
A Adhesion molecules
Siglec1
FDR 4.80E-15
Vcam1
Maea
Itgav
Cd163
B Nucleus engulfment
Mertk
Tim4
Dnase2a
FPKM
WT
KO
C Iron handling
Hmox1
Slc40a1
FDR 0.004
Trf
Tfrc
D Transcription factors
Klf1
Spic
FDR 0.051
Nr1h3
Maf
E Growth factors
Igf1
Il18
Vegfb
F Membrane receptors
Epor
Csf1r

Figure S6

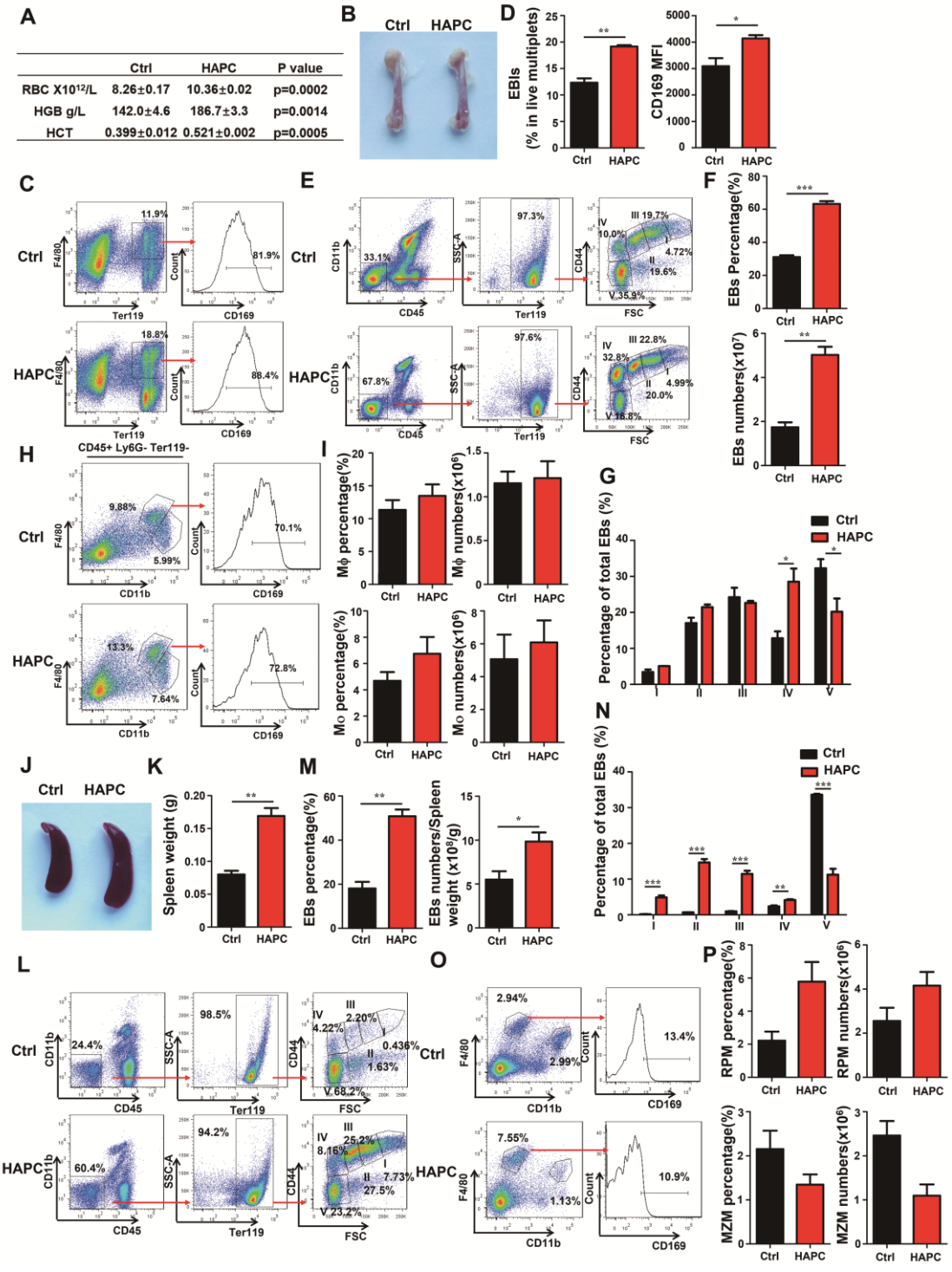
A
Ctrl HAPC P value
RBC X10^12/L 8.26±0.17 10.36±0.02 p=0.0002
HGB g/L 142.0±4.6 186.7±3.3 p=0.0014
HCT 0.399±0.012 0.521±0.002 p=0.0005
B
Ctrl HAPC
D
EBIs (% in live multiplets)
CD169 MFI
C
E
F
EBs Percentage(%)
EBs numbers(x10^7)
H
CD45+ Ly6G- Ter119-
I
Mφ percentage(%)
Mφ numbers(x10^6)
G
Percentage of total EBs (%)
J
K
Spleen weight (g)
M
EBs percentage(%)
EBs numbers/Spleen weight (x10^8/g)
N
L
O
P
RPM percentage(%)
RPM numbers(x10^6)
MZM percentage(%)
MZM numbers(x10^6)

Figure S7

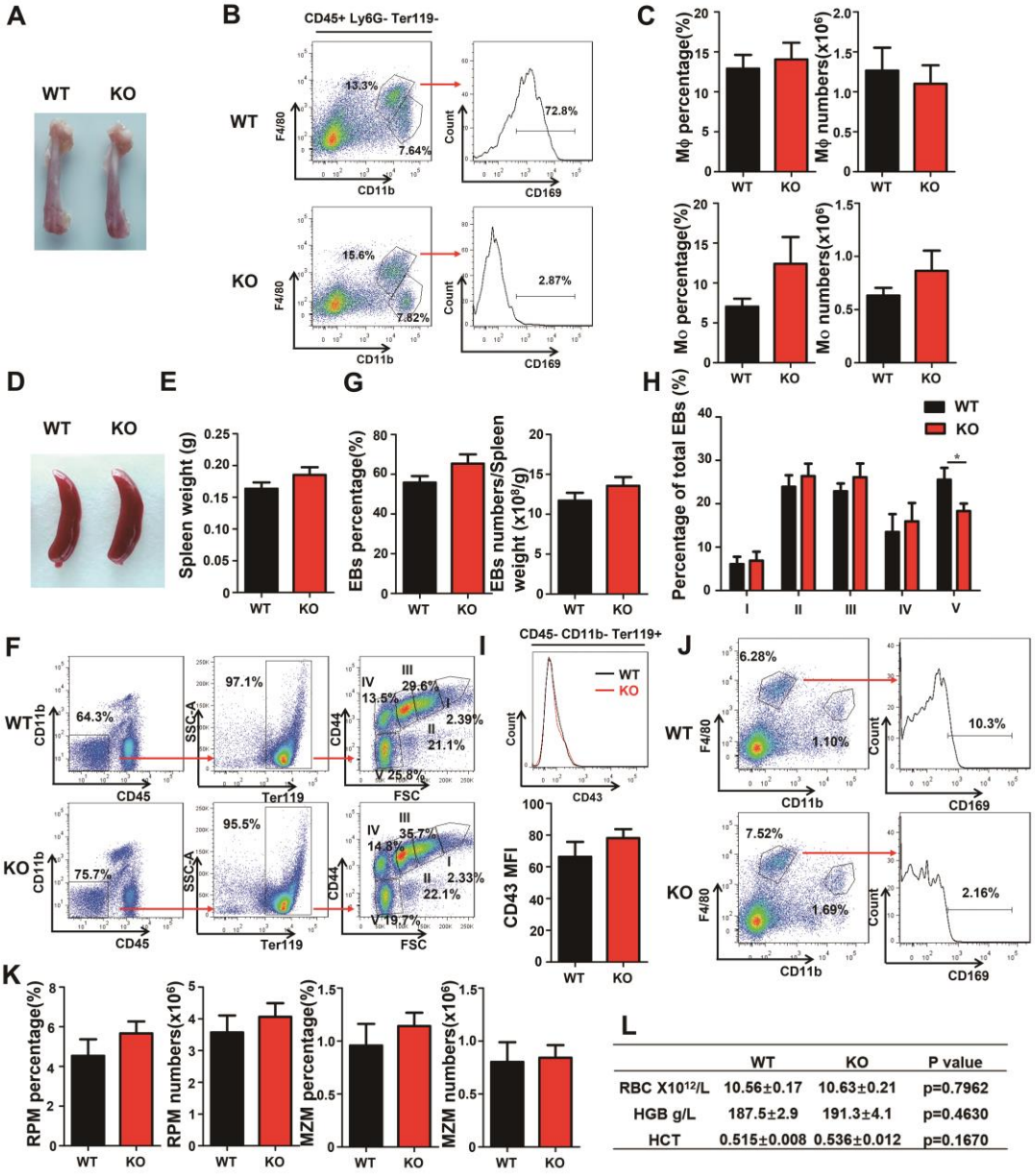

L

	WT	KO	P value
RBC X10^{12}/L	10.56±0.17	10.63±0.21	p=0.7962
HGB g/L	187.5±2.9	191.3±4.1	p=0.4630
HCT	0.515±0.008	0.536±0.012	p=0.1670

Figure S8

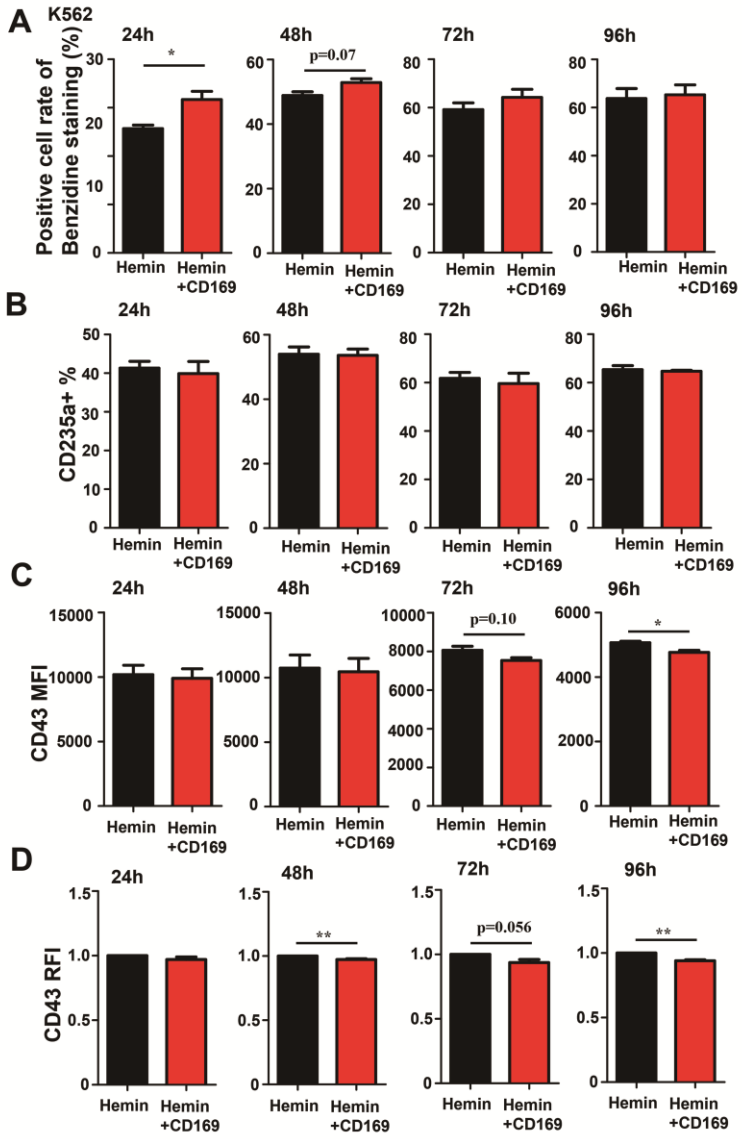
A
K562
24h
48h
72h
96h
Positive cell rate of Benzidine staining (%)
*
p=0.07
Hemin
Hemin +CD169
B
CD235a+ %
C
CD43 MFI
p=0.10
*
D
CD43 RFI
**
p=0.056